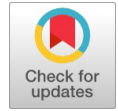


Numerical Simulation of Flow through a Centrifugal Impeller



Seralathan S, Mukesh Nadarajan, Mujibur Rahman K, Micha Premkumar T, Hariram V

Abstract: The paper reports computational results of the flow through an impeller (backward curved) of a centrifugal compressor. 3D steady state investigations are performed at off-design and design mass flow rates. The static pressure as well as stagnation pressure distribution contours and velocity vector reveals the behavior of flow through the impeller at different flow coefficients. The flow pattern observed within the impeller passage is complex and influenced by several factors. Flow through the impeller is distorted due to presence of jet and wake. As flow happens through the impeller, energy is transferred from the impeller's blades to the fluid. This creates the jet at pressure side region and wake at suction side region of the impeller. This fluid with different energy level gets mixed at the exit of the impeller causing mixing losses as well as secondary flows. These loss leads to a considerable fall in static pressure rise in the compressor and thereby affecting the overall efficiency of the centrifugal compressor. Also, existence of vortices in the flow field as flow turned from axial direction to radial is seen.

Keywords: Backward curved, centrifugal compressor, impeller, flow through impeller.

I. INTRODUCTION

The flow through a centrifugal impeller is highly complicated in nature. The efficiency of a centrifugal compressor impeller is generally high (around 90%). However, the stage efficiency is lower due to the diffuser performance. There are many parameters that affect the flow in a centrifugal impeller. The most important among them are the inlet geometry, pre-whirl, inducer, bends in the inlet system, angles at inlet and exit of the impeller blade, curvature and shape of the volute casing. The whole energy transfer in a centrifugal machine happens in the impeller and the fluid exits with increased kinetic energy as well as rise in static pressure. However, the efficiency of this transfer of energy depends on effectiveness of the above mentioned

parameters. Boundary layer effect may be appreciable since adverse pressure gradient of considerable magnitude usually exists along the channel walls.

Due to the existence of adverse pressure gradients, the boundary layer may separate disrupting the through potential flow, resulting in huge losses. Initial studies on the flow through centrifugal impeller was studied by Fowler [1], Eckardt [2, 3], and Lennemann and Howard [4]. Using a large impeller rotating at lower speed for flow investigations, Fowler [1] made extensive measurements of velocity distribution within the impeller. The measurements using a hot wire anemometer showed flow pattern having a character of jet wake flow. The velocity at suction side was lesser than the velocity at pressure side for all flow rates which was in contrast with the in-viscid flow predictions.

Dean and Senoo [5] proposed the "jet and wake" model of an impeller channel flow to account for large losses taking place at the entrance of the diffuser. They revealed that mixing of flow at the impeller's exit typically occur within a smaller radius ratio. Innoue [6] analyzed each term of the equations given by Dean and Senoo [5], and Johnson and Dean [7] to state the reasons for these theory predicting alike total pressure losses. Later, Eckardt [2, 3] with experimental results obtained by L2F velocimeter, showed the formation of the "jet-wake" structures from a nearly uniform inlet flow field to an exit flow field which was extremely distorted. A split up of sharp stable velocity gradients exist between wake and the through flow. Jet-wake structures at impeller exit, as highlighted by Hartmut Krain [8], were consequence of complex non-linear combinations involving deceleration rate of flow through impeller, flow rates, shroud cover presence, curvature and number of blades, blade exit angle, and impeller speed. Interestingly, Fowler [1] also noticed the presence of vortices in the flow field due to change of flow from axial direction to radial and the uniform flow getting into the impeller being forced towards pressure side of the flow channel due to centrifugal force, which was accelerated by the coriolis component of acceleration.

Moore and Moore [9] made a detailed analysis of the flow in a rotating radial flow passage. The presence of shear layer amid wake and jet was observed which prevented the mixing of jet and wake. The development of flow within the channel appeared similar to that in centrifugal machinery. At higher mass rate of flows, the eddy was missing and boundary layer at suction side thickened into big wake. On the other hand, at lower flow rates, eddy occurred on the pressure side, while, the boundary layer at suction side thickened into a larger wake. A detailed study on the performance of unshrouded and shrouded impellers (backward curved) of identical dimensions was done by Rajendran *et al.* [10].

Manuscript published on 30 September 2019.

*Correspondence Author(s)

Seralathan S, Department of Mechanical Engineering, Hindustan Institute of Technology and Science, Chennai, India. Email: sseralathan@hindustanuniv.ac.in

Mukesh Nadarajan, Department of Mechanical Engineering, Hindustan Institute of Technology and Science, Chennai, India. Email: revamukesh@gmail.com

Mujibur Rahman K, Department of Mechanical Engineering, Hindustan Institute of Technology and Science, Chennai, India. Email: mujibur.rahman7303@gmail.com

Micha Premkumar T, Department of Mechanical Engineering, Hindustan Institute of Technology and Science, Chennai, India. Email: tmichamech@gmail.com

Hariram V, Department of Mechanical Engineering, Hindustan Institute of Technology and Science, Chennai, India. Email: connect2hariram@gmail.com

© The Authors. Published by Blue Eyes Intelligence Engineering and Sciences Publication (BEIESP). This is an open access article under the CC-BY-NC-ND license <http://creativecommons.org/licenses/by-nc-nd/4.0/>.

On comparing with an identical unshrouded impeller, shrouded impeller gave a lesser performance in the lower flow region. Also, the stable range was narrow due to occurrence of rotating stall at the higher flow rates. According to Rajendran *et al.* [10], the velocity fluctuations in shrouded impellers were comparatively high on the shroud side, whereas it was little on the hub side. Recently, there was an increased interest on the flow patterns inside the rotating channels. Several studies (Elnashar H Amr *et al.* [11], Shimpei Mizuki *et al.* [12]) were performed by researchers to understand the fundamentals behind the flow in centrifugal impeller. As pointed out by Hartmut Krain [8], numerical simulations help in better understanding of the flow physics involving flow through a centrifugal impeller. Therefore, the focus of this study is to analyze numerically the flow through an impeller (backward curved; $\beta_2 = 65^\circ$) of a centrifugal compressor under steady state conditions at off-design and design flow coefficients.

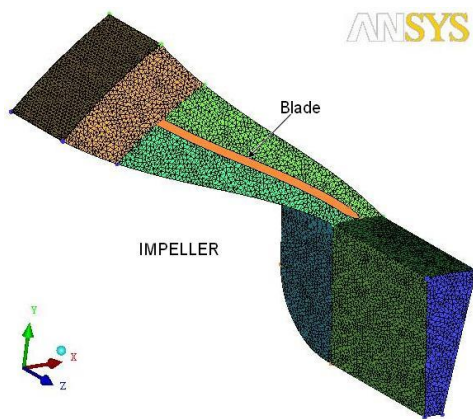


Fig. 1. Computational domain

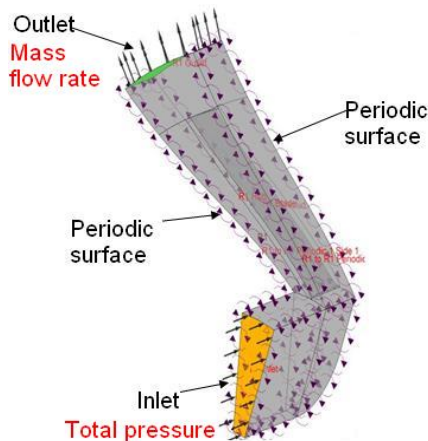


Fig. 2. Boundary conditions

II. NUMERICAL APPROACH

A centrifugal compressor (low-specific speed) chosen for this investigations and its detail is listed in Table I. As experimental data [13] is on hand, the same is chosen to model and investigate numerically. Geometric model deployed for simulation consists of a shrouded impeller with blade. On the basis that flow is periodic in all impeller's blade passages, the concept of single passage approach (i.e., one

blade passage) is deployed to model the configuration instead of modeling the entire impeller geometry. This approach saves enormous computational resources and time. The point by point method is adopted to design the impeller blade using ANSYS ICEMCFD. The fluid domain at inlet is kept at the forefront by about half the chord length of blade and the domain's outlet is kept at a distance of one fourth of the blade chord length. During meshing, unstructured grid is generated using tetrahedral elements for the entire computational domain. At least six fine prism shaped cell are deployed nearer to wall to facilitate better resolution within the boundary layer as illustrated in Fig. 1. ANSYS ICEMCFD is utilized to perform modeling and meshing of fluid domain.

Table-I: Geometric data and operating conditions

| | |
|--|--------------|
| Pressure rise, ΔP | 200 mm Water |
| No. of blades, Z | 24 |
| Outlet blade angle, β_2 | 65° |
| Blade width, b [Width at exit, b_2 is equal to at inlet, b_1] | 50 mm |
| Inlet blade angle, β_1 | 35° |
| Diameter at inlet of impeller, d_1 | 280 mm |
| Diameter ratio, d_1/d_2 | 0.51 |
| Diameter at exit of impeller, d_2 | 550 mm |
| Speed, N | 1800 rpm |
| Mass flow rate, m | 1.003 kg/s |

Table-II: Grid independency study ($m = 0.04198$ kg/s)

| Element count | Energy coefficient, ψ | |
|---------------|----------------------------|-----------------------------------|
| | Standard $k-\omega$ | $k-\omega$ shear stress transport |
| 397471 | 0.948 | 0.9894 |
| 500961 | 0.967 | 1.028 |
| 776868 | 1.001 | 1.061 |

Table-III: Turbulence model study

| Flow coefficient, $\Phi = C_m/U$ | Flow rate (kg/s) | Energy coefficient, ψ | | |
|----------------------------------|------------------|----------------------------|-----------------------------------|------------|
| | | Turbulence models | | Expt. [13] |
| | | Standard $k\omega$ | $k-\omega$ shear stress transport | |
| 0.19 (design) | 0.04198 | 1.001 | 1.061 | 1.08 |

Grid independency test (refer Table II) is done to ensure independency of the result irrespective of mesh generated. Based on these, the element count (prism and tetrahedral) in the fluid domain is 776868 elements. Two equation models namely, $k-\omega$ shear stress transport and standard $k-\omega$ turbulence model is utilized to perform turbulence model study as listed in Table III. The obtained data are verified with the experimental result [13]. Since data based on $k-\omega$ SST model is closer, further studies are performed using $k-\omega$ SST turbulence model [14-17]. Figure 2 depicts definition of each boundary. Computational domain inlet is placed 105 mm ahead from eye of the impeller. This approach ensures that inlet boundary conditions aren't impaired by the back pressure of impeller's blades. Rotating frame of reference is specified for the entire

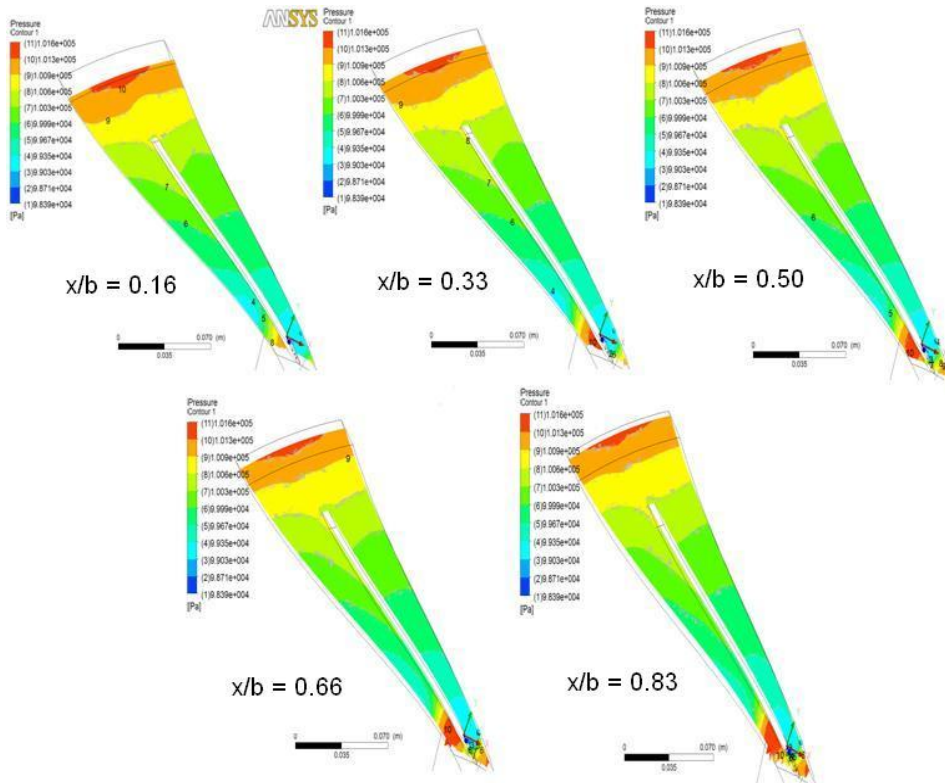


Fig. 3. Static pressure distribution contours, $\Phi = 0.25$

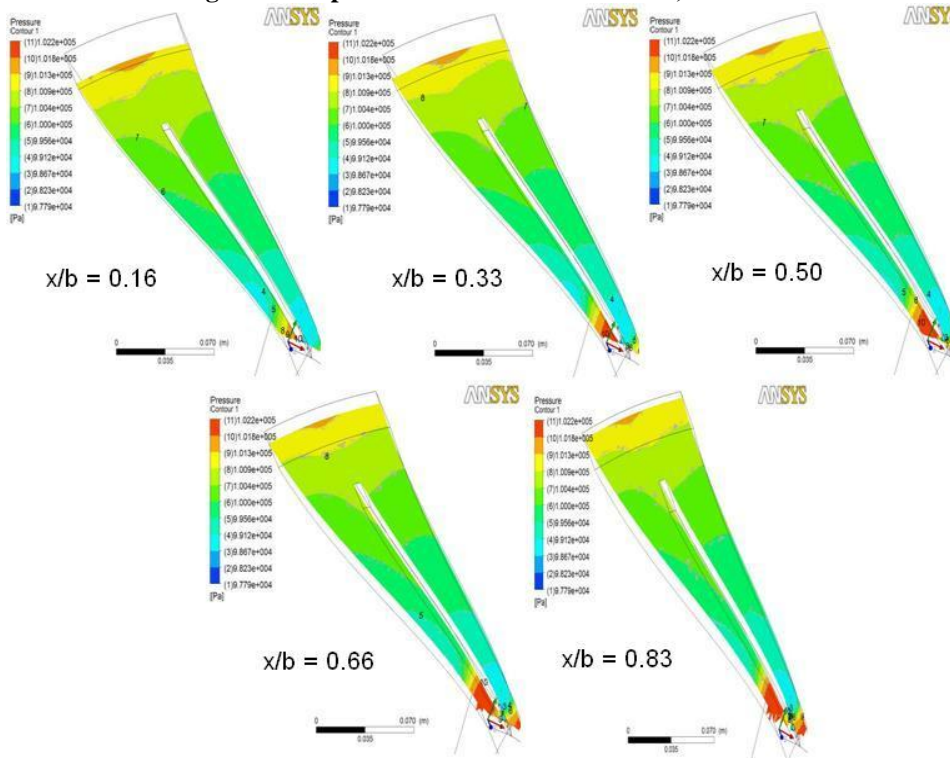


Fig. 4. Static pressure distribution contours, $\Phi = 0.19$

computational domain. Total pressure in stationary frame is an inlet boundary condition in which reference pressure mentioned is 101.325 kN/m². As a result, at inlet, zero Pa is the relative total pressure. The fluid mentioned is air at 25°C. k- ω SST turbulence model is chosen owing to its accuracy and robustness, and turbulence intensity is mentioned to be 1% (with medium level). Rotational periodic boundary is mentioned for the side walls of impeller domain. The outlet is mentioned as mass flow rate. The impeller is rotating with an

angular velocity same as the domain. With reference to relative frame of reference, it is stationary and it is mentioned with wall boundary conditions. The wall is mentioned with no-slip conditions. Wall roughness is ignored and assumed to be smooth. Numerical studies are performed with FVM based CFD code, ANSYS CFX. The governing equations are

Numerical Simulation of Flow through a Centrifugal Impeller

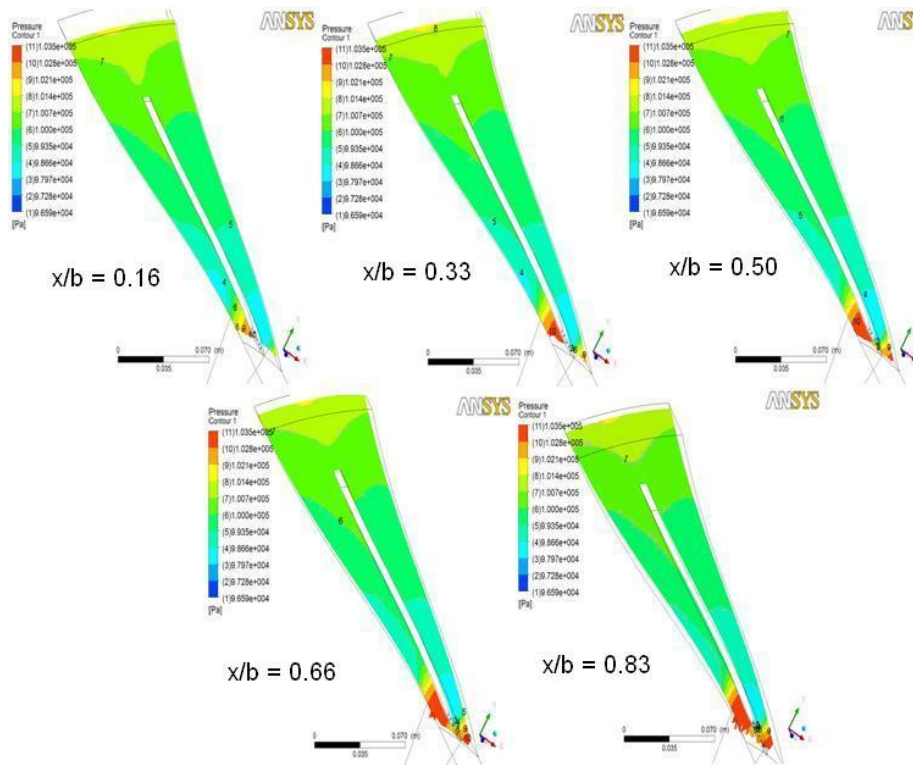


Fig. 5. Static pressure distribution contours, $\Phi = 0.15$

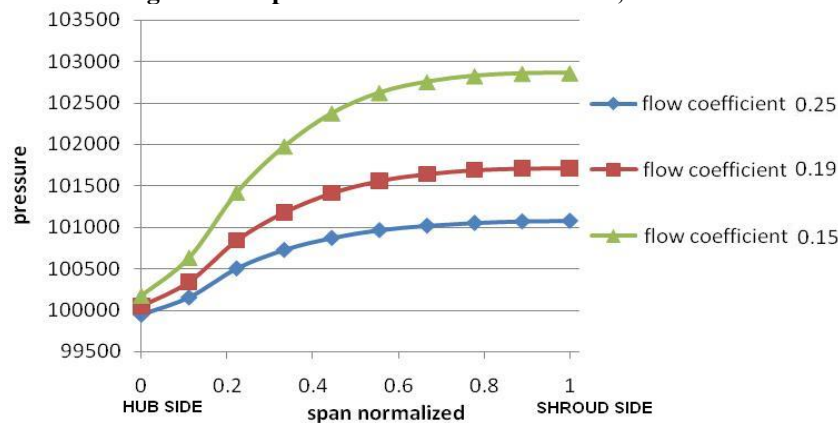


Fig. 6. Span wise static pressure distributions

resolved under steady state solutions till the residuals got converged. The target variable monitored at impeller outlet is mass averaged pressure. The RMS residuals convergence conditions of all governing equations are set as 10^{-4} .

III. RESULTS AND DISCUSSION

The numerical investigation outcome for flow coefficient viz., $\Phi = 0.15$ and 0.25 (off-design), $\Phi = 0.19$ (design), are discussed. Turbo surface is introduced to elucidate the flow physics of flow within the impeller. It is introduced at five axial locations namely 16%, 33%, 50%, 66% and 83% between shroud and hub along axial plane in-line with impeller width.

Based on this, contours of total pressure and static pressure are illustrated for non-dimensionalized axial distance $x/b = 0.85$ (shroud), 0.66 , 0.50 , 0.33 , and 0.16 (hub) and it is interpreted here. Static pressure rises with radius due to the flow diffusion. This is revealed in static pressure distribution contours, as seen in Figs. 3 to 5, for flow through centrifugal impeller at $\Phi = 0.25$, 0.19 and 0.15 . As the

impeller rotates, the energy passed onto the fluid is realized by rise in its kinetic energy which transformed itself into static pressure as it moves along the radius ratio. Also, the static pressure distributions observed in the circumferential directions is nearly uniform.

This is revealed in axial direction namely, $x/b = 0.16$ (hub) to $x/b = 0.83$ (shroud). As can be observed at Fig. 6, at $\Phi = 0.15$, the maximum static pressure rise is realized by the impeller. There is a slight drop in the static pressure for $\Phi = 0.25$ when evaluated against design flow coefficient. However, static pressure varies in the region of impeller exit width and the pressure is increasing from hub side to shroud side. It is to be noted that static pressure rise is less for higher flow coefficient and static pressure increases as the mass flow rates decrease. Also, the presence of vortices in the flow field as flow turned from axial direction to radial is seen (refer Fig. 11). Contour of stagnation pressure distributions for flow through centrifugal impeller at different flow coefficients are illustrated in Figs. 7 to 9.

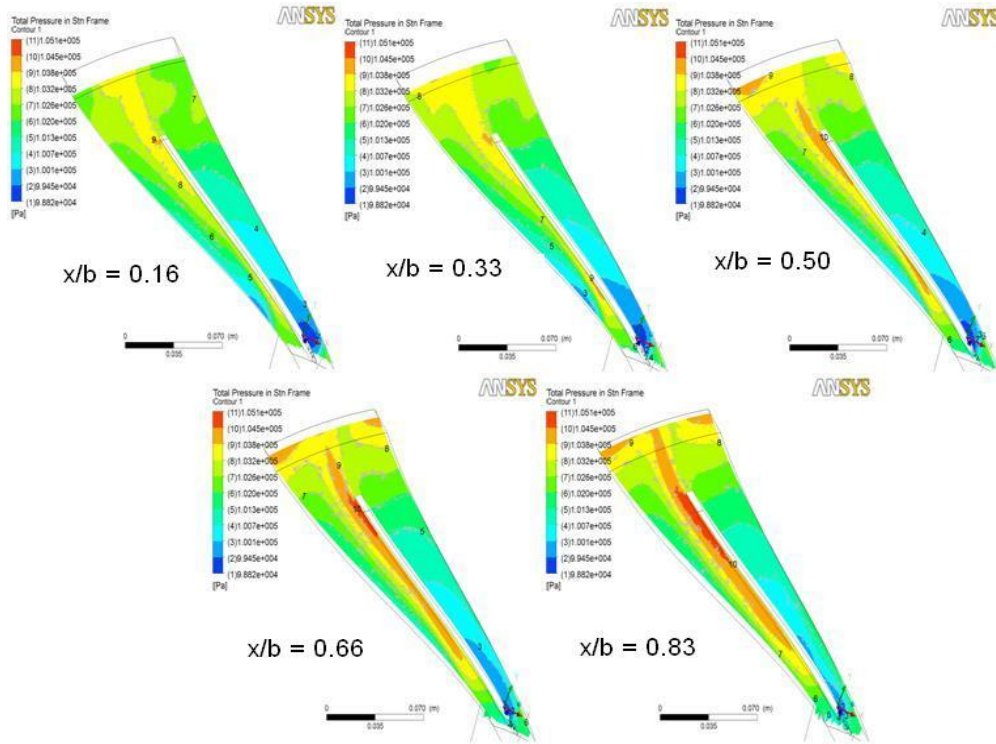


Fig. 7. Stagnation pressure distribution contours for $\Phi = 0.25$

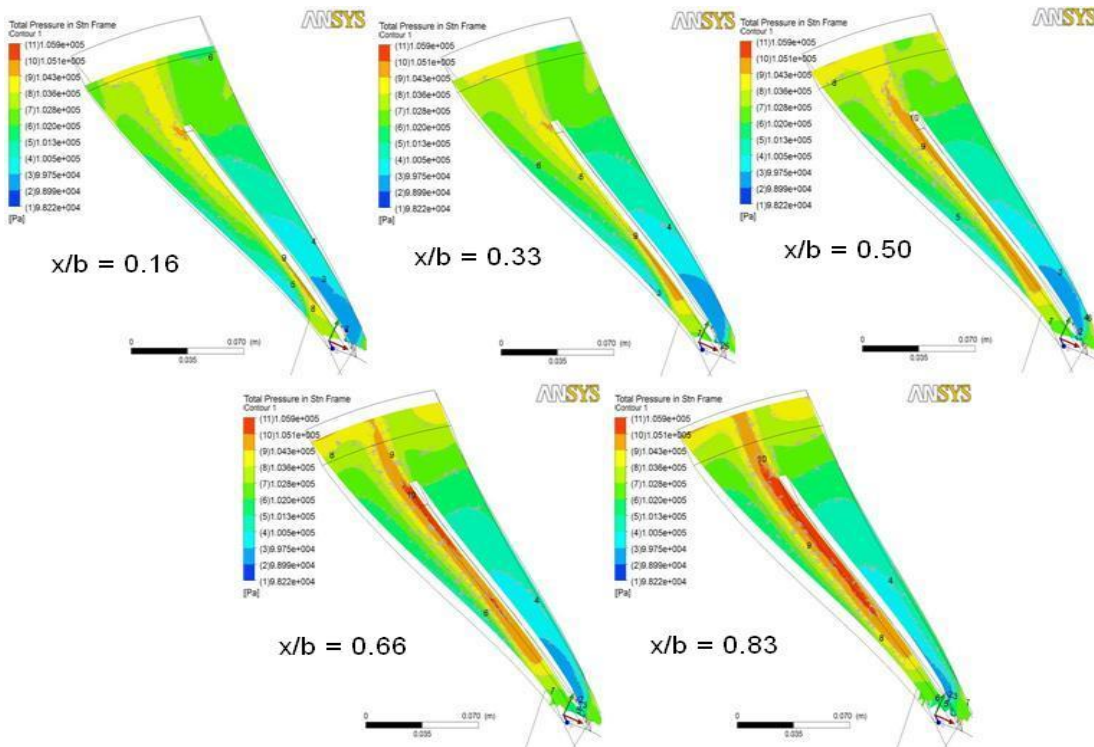


Fig. 8. Stagnation pressure distribution contours for $\Phi = 0.19$

Stagnation pressure increases as radius ratio increases. As the flow coefficient decreases, the value of stagnation pressure increases. The total pressure distribution at axial location $x/b = 0.20$ is higher than that nearer to hub and shroud which is reflected for all flow coefficients. The span wise distributions of absolute velocity distribution are shown in Fig. 10.

The presence of separated zones at impeller exit, which limits the impeller diffusion, was investigated by various researchers. Figure 11 shows the velocity vector plot at various flow coefficients. As flow happens through the

impeller, the energy is transferred from the blade to fluid. This creates the “jet” at pressure side and “wake” at suction side region of the impeller. As can be observed in Fig.11, the separated zone namely, the jet and wake region is clearly visualized in the flow through impeller as well as at the impeller exit.

Similarly, non-uniformities are seen

between the axial directions (viz., hub-to-shroud) plus in the circumferential directions (viz., blade-to-blade).

The fluid with varied energy levels mixes at the impeller exit. This mixing causes significant loss in total pressure.

Moreover, wake formation is large at higher mass flow rates resulting with larger total pressure loss which includes mixing and frictional losses. It is understood that radial

component inside the wake is small and the absolute flow angle with reference to tangential direction is also small resulting the flow to take a larger path causing larger frictional losses. This is in contrary to the jet which follows a shorter path resulting in less frictional losses. This jet-wake phenomenon is responsible for difference in total energy at impeller exit.

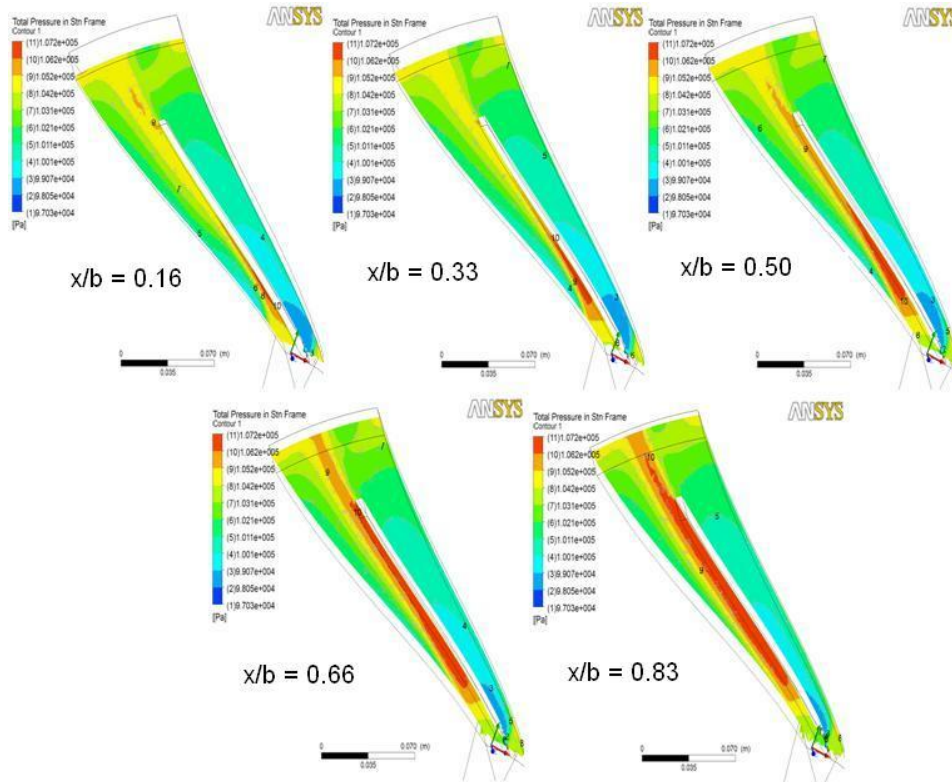


Fig. 9. Stagnation pressure distribution contours for $\Phi = 0.15$

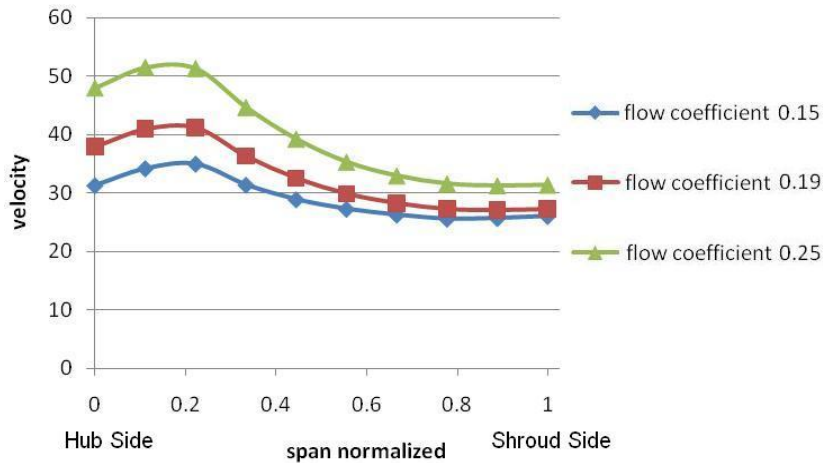


Fig. 10. Span wise distribution of absolute velocity

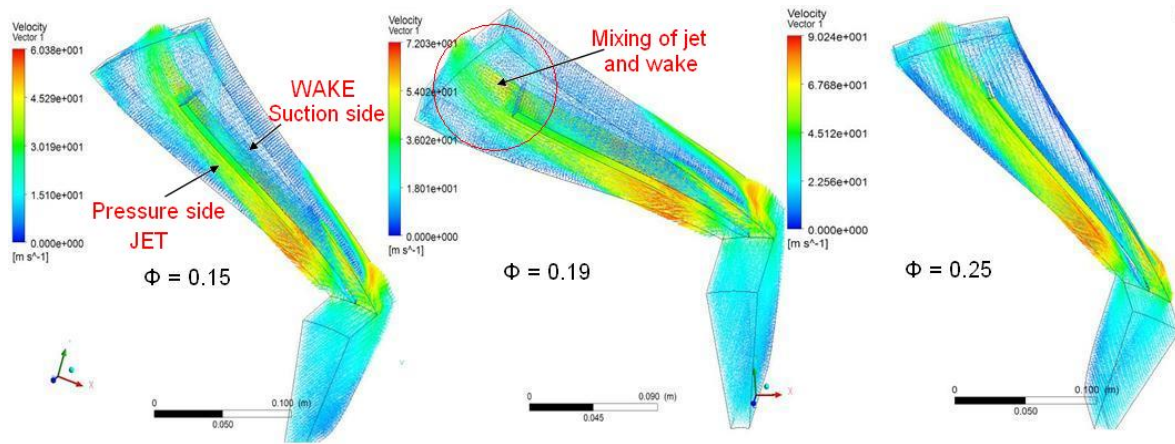


Fig. 11. Velocity vectors

IV. CONCLUSION

The numerical investigation on flow through the centrifugal impeller of the centrifugal compressor is analyzed at various flow coefficients involving off design ($\Phi = 0.15$, and 0.25) and design ($\Phi = 0.19$) conditions. The key outcomes of are listed below:

- Fluid with high kinetic energy, viz., the jet and fluid with low kinetic energy, i.e., wake are observed on pressure side and suction side of the impeller respectively.
- Mixing phenomenon is observed at impeller exit.
- Nearly uniform static pressure distributions are observed in the axial direction from hub-to-shroud.
- Static pressure rise gradually from impeller eye till impeller exit due to flow diffusion.
- Presence of vortices in the flow field as flow turned from axial direction to radial.
- Static and stagnation pressure increases with decrease in flow coefficients.

REFERENCES

1. H. S. Fowler, "The distribution and stability of flow in rotating channel", ASME Journal of Engineering for Power, vol. 90, 1968, pp. 229 - 236.
2. D. Eckardt, "Instantaneous measurements in the jet-wake discharge flow of a centrifugal compressor impeller", ASME Journal of Engineering for Power, 1975, pp. 337 -346.
3. D. Eckardt, "Detailed flow investigations within a high speed centrifugal compressor impeller", ASME Journal of Fluid Engineering, 1976, pp. 390 - 402.
4. E. Lennemann and J. H. G. Howard, "Unsteady flow phenomena in rotating centrifugal impeller passages", ASME Journal of Engineering for Gas Turbines and Power, vol. 92(1), 1970, pp. 65-71.
5. R.C. Dean JR and Y. Senoo, "Rotating wakes in vaneless diffuser", Journal of Basic Engineering, 1960, pp. 563 - 574.
6. M. Inoue, "Radial vaneless diffusers: a re-examination of the theories of Dean and Senoo and of Johnston and Dean", ASME Journal of Fluids Engineering, vol. 105, 1983, pp. 21-27.
7. J. P. Johnston and R.C. Dean JR, "Losses in vaneless diffusers of centrifugal compressors and pumps - analysis, experiment and design", ASME Journal of Engineering for Power, 1966, pp. 49 - 62.
8. Hartmut Krain, "Review of Centrifugal Compressor's Application and Development", ASME Journal of Turbomachinery, vol. 127(1), 2005, pp. 25-34.
9. J. Moore, and J.G. Moore "Calculations of three-dimensional viscous flow and wake development in a centrifugal impeller", Proceedings of ASME CP Performance Prediction of Centrifugal Pumps and Compressors, 1980, New York, pp. 61-67.

10. R. Rajendran, S. Ramamurthy and P. Mohanan, "Aerodynamic investigation of flow through a centrifugal compressor stage", Proceedings of the 12th Asian Congress of Fluid Mechanics, August 18-21 2008, Daejeon, Korea, 4 pages.
11. Elnashar H Amr, Eldalil M Khaled, Hashim A Ali and Abdelrahman M Mohamed, "Theoretical and experimental study of centrifugal compressor impellers", Proceedings of ICFDP9: Ninth International Congress of Fluid Dynamics & Propulsion, December 18-21,2008, Alexandria, Egypt, Paper No. ICFDP9-EG-243.
12. Shimpei Mizuki, Ichiro Arigo and Ichiro Watanabe, "A study on the flow mechanism within centrifugal impeller channels", ASME Paper No. 75-GT-14, V01AT01A013 14 pages.
13. K. Sankaran, "Flow Studies at the exit of Centrifugal Impeller", Ph. D. Thesis Report, Thermal Turbomachines Laboratory, Department of Mechanical Engineering, Indian Institute of Technology Madras, India, 1985.
14. M. Govardhan, and S. Seralathan, "Effect of forced rotating vaneless diffusers on centrifugal compressor stage performance", Journal of Engineering Science and Technology, Vol. 6. No. 5, 2011, pp. 558 - 574.
15. S. Seralathan and D. G. Roy Chowdhury, "Performance enhancement of a low-pressure ratio centrifugal compressor stage with a rotating vaneless diffuser by impeller disk", Journal of Applied Fluid Mechanics, vol. 9, No.6, 2016, pp. 2933-2947.
16. S. Seralathan and D. G. Roychowdhury, "Numerical studies on the effect of diffuser rotational speeds on low pressure ratio centrifugal compressor performance", Journal of Applied Fluid Mechanics, vol. 10, No. 3, 2017, pp. 785-799.
17. Chaina Ram, Seralathan Sivamani, T. Micha Premkumar, and Hariram Venkatesan. "Computational study of leading edge jet impingement cooling with a conical converging hole for blade cooling", ARPN Journal of Engineering and Applied Sciences, vol. 12, Issue. 22, 2017, pp. 6397-6406.